

A PROOF-OF-PRINCIPLE ECHO-ENABLED HARMONIC GENERATION EXPERIMENT AT SLAC*

M. Dunning[†], E. Colby, Y. Ding, J. Frederico, S. Gilevich, C. Hast, K. Jobe, D. McCormick, J. Nelson, T.O. Raubenheimer, K. Soong, G. Stupakov, Z. Szalata, D. Walz, S. Weathersby, M. Woodley, D. Xiang, SLAC, Menlo Park, CA, USA
 J. Corlett, J. Qiang, G. Penn, S. Prestemon, R. Schlueter, M. Venturini, W. Wan
 LBNL, Berkeley, CA, USA
 P-L. Pernet, EPFL, Lausanne, Switzerland

Abstract

In this paper we describe the technical design of an ongoing proof-of-principle echo-enabled harmonic generation (EEHG) experiment at the Next Linear Collider Test Accelerator (NLCTA) at SLAC. We present the design considerations and the technical details of the experiment.

INTRODUCTION

Recently a new method, entitled echo-enabled harmonic generation, was proposed for generation of high harmonics using the beam echo effect [1, 2]. In an EEHG free electron laser (FEL), an electron beam is energy modulated in a modulator and then sent through a dispersive section with a high dispersion strength. After this first stage, the modulation obtained in the modulator is macroscopically washed out, while simultaneously introducing complicated fine structure (separated energy bands) into the phase space of the beam. A second laser is used to further modulate the beam energy in a second modulator. After passing through a second dispersive section, the separated energy bands will be converted into current modulation and the echo signal then occurs as a re-coherence effect caused by the mixing of the correlations between the modulation in the second modulator and the fine structures in the beam.

The EEHG scheme has a remarkable up-frequency conversion efficiency; it has been shown that the EEHG FEL scheme may allow generation of soft x-rays directly from a UV seed laser in a single stage [3]. In order to confirm the physics behind the EEHG technique and benchmark the theory, a proof-of-principle EEHG experiment was planned at SLAC. The experiment is now in a commissioning stage and the preliminary results are reported in a separate paper of these proceedings [4]. In this paper we present the design considerations and the details of the experiment setup.

LAYOUT

The layout of the echo experiment at SLAC is schematically shown in Fig. 1. The experiment is based on the existing NLCTA facility [5]. At the NLCTA, the electron beam is generated in a photocathode rf gun and is boosted to 60 MeV in an x-band linac (X-band 1). After passing through

a chicane (termed *chiane minus one*, or C-1), the beam is typically used for high-gradient rf structure testing, or can be used for various experiments including the SLAC E163 laser acceleration experiments [6].

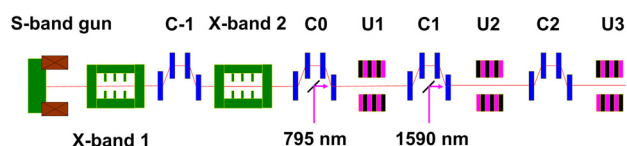


Figure 1: Layout of the EEHG experiment at the NLCTA.

In order to support the proof-of-principle echo experiment at the NLCTA, another x-band structure (X-band 2) was added downstream of C-1 to further accelerate the beam to 120 MeV. The main components of the echo beam-line are 3 chicanes (C0, C1 and C2), 3 undulators (U1, U2 and U3) and quadrupole magnets for beam matching and focusing. C0 is a mini-chicane used to generate an orbit bump so that a mirror can be inserted for laser injection. The beam is first energy modulated in U1 with a 795 nm laser and then passes through C1, the first dispersive section. The beam is again energy modulated in U2 with a 1590 nm laser, then C2 is used to convert the separated energy bands into separated current bands. The density modulated beam then generates coherent harmonic radiation in U3. Four trim quads are used each in C1 and C2 to correct the unwanted R_{51} and R_{52} caused by field errors and higher order field components of the dipole magnets [7].

DESIGN CONSIDERATIONS

Since the first laser is used only to generate separated energy bands, the harmonic number is better described by $n = \lambda_2/\lambda_r$, where λ_2 is the wavelength of the second laser and λ_r is the wavelength of the harmonic radiation generated in U3. This experiment aims at generating a moderate harmonic ($n = 5$ and $n = 7$) of the second laser (the experiment is termed ECHO-7 in short). In order to avoid constructing an in-vacuum UV spectrometer, a relatively long wavelength laser ($\lambda_2 = 1590$ nm) is used in the second modulator so that the 5th and 7th harmonic are above the VUV range. The 1590 nm laser is produced by an optical parametric amplifier (OPA) system pumped with the 795 nm laser. The main parameters of the EEHG experiment are listed in Table. 1.

* Work supported by US DOE contracts DE-AC02-76SF00515.

[†] mdunning@slac.stanford.edu

Table 1: Main parameters of the EEHG experiment.

Beam energy	120 MeV
Normalized emittance	8 mm-mrad
Bunch charge	25 pC
Laser wavelength in U1	795 nm
Laser wavelength in U2	1590 nm
Slice energy spread	2-10 keV
$N_p \times \lambda_u$ for U1	10×3.3 cm
$N_p \times \lambda_u$ for U2	10×5.5 cm
$N_p \times \lambda_u$ for U3	10×2 cm
Peak energy modulation in U1 and U2	10-40 keV
R_{56} for C1 and C2	1.0-9.0 mm
Radiation wavelength in radiator	318 and 227 nm

U1 and U2 have fixed gaps while U3 is designed to be adjustable in gap so that it can be tuned to the 5th or 7th harmonic of the second laser.

Because EEHG requires a long term memory of the beam phase space, it is in general sensitive to diffusion effects. For a low energy beam, typically the quantum diffusion from incoherent synchrotron radiation and incoherent undulator radiation is not a serious issue and the second order effect from the emittance (particles with different betatron amplitude have different path lengths) is a major concern. The lattice is carefully designed to have a small β_{max}/β_{min} to mitigate the smearing from second order transport effects. For the 7th harmonic case, the longitudinal phase space at the entrance to U3 is simulated with elegant [8] and is shown in Fig. 2 for two different values of the transverse emittance. In order to quantify the smearing effect, a bunch with vanishing length was tracked through the echo beam line; at the beamline exit the bunch length is increased to approximately 80 nm. The simulations indicate that the current beam quality (about 8 mm-mrad emittance) is adequate for generating the 7th harmonic, but improved beam quality is needed if one plans to generate higher harmonics. Future plans are to replace the photocathode and drive laser and modify C-1, to achieve an emittance of approximately 2 mm-mrad. This will enable generation and measurement of the 15th harmonic of the second laser in U3 (3rd harmonic of the fundamental radiation which is tuned to the 5th harmonic of the second laser).

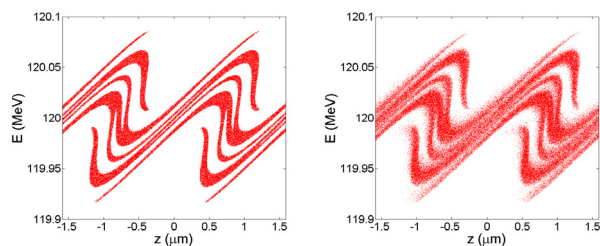


Figure 2: Phase space at the entrance to U3 for different beam emittances: 1 mm mrad (left); 8 mm mrad (right).

In addition to second order effects from the transverse emittance, several other effects could wash out the fine structure in the beam, including misalignment of the quads, field errors of the dipoles, and the non-zero field integral of the undulators. Extensive simulations have been performed to set the corresponding tolerances. For instance, the beam was tracked in simulation through a chicane of which the dipoles had 0.5% field errors. The simulated phase space after C2 is shown in Fig 3, where it is shown that the fine structure is nearly completely washed out without trim quad correction. Analysis shows that the smearing effect is from the unwanted $x - z$ coupling from the non-zero R_{51} and R_{52} caused by the field errors. For this specific case, we have $R_{51} \approx 2.4 \times 10^{-4}$, $R_{52} \approx 2.9 \times 10^{-4}$ and the bunching factor is about 0.2%. Considering the fact that at the entrance to the chicane $\sigma_x \approx 0.3$ mm and $\sigma_{x'} \approx 0.13$ mrad, the $x - z$ coupling may wash out any structure that is finer than $2\pi\sqrt{(\sigma_x R_{51})^2 + (\sigma_{x'} R_{52})^2} \approx 500$ nm.

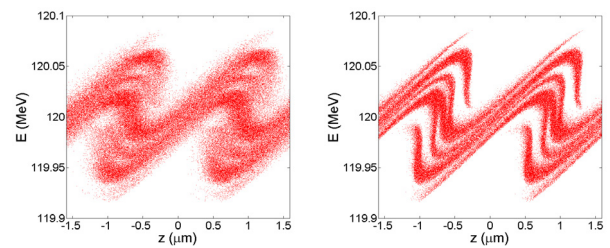


Figure 3: Longitudinal phase space at the exit of C2 with (right) and without (left) trim quad correction when 0.5% field error is present.

In our design the dipoles are powered by the same power supply, but due to mechanical differences, the field integral has some error. In order to reduce the field errors to within 0.1%, the trim coils are integrated with the main windings of the dipoles so that one can finely adjust the trim coil current to compensate for the field differences from the main windings. Furthermore, two trim quads are also used in the chicane to correct the field error and the higher order field components. Simulation shows that by empirically adjusting the strength of the trim quads, one can greatly reduce the R_{51} and R_{52} so that the $x - z$ coupling effect is significantly mitigated. For the example above, when the trim quads were adjusted to proper settings, R_{51} and R_{52} were reduced by one order of magnitude and the fine structure was restored after C2 (see right plot of Fig. 3).

The beam will receive a kick after exiting the undulator if the first field integral is non-zero. Similarly the beam will have an offset after exiting the undulator if the second field integral is non-zero. The effect of the kick is similar to a dipole that causes $x - z$ coupling which tends to wash out the fine structure in phase space. In order not to significantly affect the EEHG performances, the specifications for the first field integral of the undulators is set to 10 G-cm, which corresponds to a kick of about $25 \mu\text{rad}$. The second field integral is set to 1000 G-cm^2 which corresponds to an offset of about $25 \mu\text{m}$.

Diagnostics for measuring the echo signal are also a major concern. While backward transition radiation in the UV range can still be generated with an optical transition radiation (OTR) foil, it is not suitable for coherent radiation generation when the electron beam transverse size is comparable to or larger than $\gamma\lambda_r$. The transverse beam size does not affect the phase of the radiation if it is observed on-axis in far field. However, the OTR intensity peaks at $1/\gamma$. So if the radiation is measured at this angle, the transverse size of the beam will affect the phase of the radiation, and thus the radiation intensity is significantly suppressed when beam size is larger than $\gamma\lambda_r$. For our case the beam size is about one order of magnitude larger than $\gamma\lambda_r$ when $\lambda_r = 227$ nm, and analysis shows that we will measure few coherent photons with an OTR foil. As an alternative, undulator radiation intensity peaks in the forward direction and is much less sensitive to the transverse beam size. A third undulator was installed for generating coherent radiation at 318 nm and 227 nm.

EXPERIMENT SETUP

The beam line was completed in April 2010 and presently the experiment is in the commissioning stage. Some preliminary results are presented in these proceedings [4]. Here we describe some details of the experiment setup.

An image of the second chicane, C2, after installation is shown in Fig. 4, where the blue elements are the dipoles and orange elements are the trim quads for field error correction. The trim quads can be moved remotely so that no beam kick results when the bend angle is changed. Two mirrors were installed in the center of the chicane: one is used to reflect out the upstream laser so that the laser power and mode quality can be monitored during the experiment, and the other is used to inject the downstream laser. By reflecting out the laser, the background in the echo signal measurement is also effectively reduced.



Figure 4: Image of C2 after installation.

The second undulator, U2, is shown in Fig. 5. OTR screens are installed immediately upstream and downstream of each undulator, which are used for laser-electron spatial overlap. Another OTR screen immediately downstream of each undulator is used to reflect out the laser and undulator radiation for temporal synchronization; the radiation is detected by a fast photodiode (2 GHz bandwidth)

and is analyzed with an oscilloscope (2.5 GHz bandwidth). By referencing the signals to an external trigger, the laser and beam can be synchronized to within approximately 30 ps. More precise timing is done by using a fast scanning delay stage and measuring the coherent radiation enhancement that is produced when the beam is bunched by each modulator and dispersive section.



Figure 5: Image of U2 after installation.

SUMMARY

In order to confirm the physics behind the EEHG technique and benchmark the theory, a proof-of-principle EEHG experiment is underway at the NLCTA at SLAC. It has gone from the design stage into commissioning within one year. After the 5th and 7th harmonics (227 nm and 318 nm) are measured, beamline upgrades are planned to enable the measurement of the 15th harmonic (106 nm).

ACKNOWLEDGEMENTS

We thank C. Adolphsen, J. Byrd, A. Chao, P. Emma, W. Fawley, J. Frisch, G. Hays, Z. Huang, H. Loos, H. Nuhn, F. Wang, X. Wang, W. White, J. Wu and A. Zholents for helpful discussions, comments and commissioning assistances.

REFERENCES

- [1] G. Stupakov, Phys. Rev. Lett, 102 (2009) 074801.
- [2] D. Xiang and G. Stupakov, Phys. Rev. ST-AB, 12 (2009) 030702.
- [3] D. Xiang and G. Stupakov, "Coherent soft x-ray generation in the water window with the EEHG scheme", Proceedings of PAC'09.
- [4] D. Xiang *et al.*, "Preliminary results of the echo-seeding experiment ECHO-7 at SLAC", These proceedings, (2010).
- [5] "NLC test accelerator conceptual design report", SLAC-Report-411, (1993).
- [6] C. Sears *et al.*, Phys. Rev. ST-AB, 11 (2008) 101301.
- [7] D. Xiang and G. Stupakov, "Tolerance study for the echo-enabled harmonic generation free electron laser", Proceedings of PAC'09, (2009); see also SLAC-PUB-13644.
- [8] M. Borland, "Elegant: A flexible SDDS-compliant code for accelerator simulation," Advanced Photon Source LS-287, September, (2000).